

Interatomic force fields for silicon microclusters

James R. Chelikowsky and Keith M. Glassford

*Department of Chemical Engineering and Materials Science, Minnesota Supercomputer Institute,
University of Minnesota, Minneapolis, Minnesota 55455*

J. C. Phillips

AT&T Bell Laboratories, Murray Hill, New Jersey 07974

(Received 22 January 1991)

We define an interatomic potential for silicon. As with previous work, this potential is based on bulk interactions that are adjusted to describe "covalent \rightarrow metallic" phase transitions instead of small-amplitude atomic vibrations. It includes the transfer of bond strength from dangling bonds to back bonds. However, this potential has been slightly modified to reduce its range. With the modified potential we determine the energies and structural properties of Si_n , where $n \leq 30$. For $n \leq 10$, we find this potential leads to a significant improvement over previous work for both the binding energies and the bond lengths of these clusters when compared with quantum-mechanical methods. For $10 < n \leq 20$ we find as before, and in agreement with experiment, that Si_n clusters follow an icosahedral pentagonal growth sequence with $n = 13$ and 19 being special structures. For $20 < n \leq 30$ we find this growth sequence is weakened, but a general pentagonal sequence is retained. We examine the role of back-bond strengthening by varying the strength of the corresponding interaction. We find that with increasing back-bond strength a "first-order" phase transition occurs that mimics the bulk "covalent \rightarrow metallic" transition. The ability to vary this interaction will allow us to examine intrinsic differences in the nucleation of covalent versus metallic clusters.

I. INTRODUCTION

Classical interatomic force fields offer many practical advantages over first-principles quantum calculations in the study of the structure and properties of matter containing more than a few atoms. Such fields are well known in the study of interactions of closed-shell atoms in terms of central forces. However, open-shell atoms may interact through mixtures of central two-body and directional, or many-body, valence forces. A particularly interesting case is silicon, which has a rich phase diagram containing both metallic and semiconductive phases. Cohen and co-workers¹ have calculated the equations of state of these phases from first-principles pseudopotentials with great accuracy. They have been successful in predicting high-pressure phases as well as superconducting ones. Their work has stimulated many recent efforts²⁻¹³ to generate classical force fields which can reproduce their equations of state and simultaneously predict other properties as well. We obtained^{14,15} the best fit to date to their equations of state by using a "non-classical" angular dependence on bond angle. This dependence scaled as $\sim \cos(3\theta)$, instead of the usual form $\cos(\theta)$, where θ is the bond angle. Our approach leads to both an angular and a radial cutoff and demonstrated the novel and profound conceptual content of the pseudopotential work.¹

Atomic clusters are subject to strong surface forces generated by broken, or dangling, bonds which transfer bond strength to back bonds. We found it necessary to

include these forces to obtain compact structures in "reasonable" agreement with molecular-orbital^{16,17} and pseudopotential results^{18,19} for Si_n clusters with $3 \leq n \leq 10$. Our chief aim was to use this force field to calculate cluster structures with $n > 10$. We achieved this aim¹⁵ and succeeded in explaining anomalies²⁰ in chemical reactivity of Si_n clusters in terms of pentagonal (icosahedral) structures.

At present there are serious unresolved questions²⁰⁻²³ about the reactivities of Si_n clusters with $n \geq 30$ which are obtained in experiments with different time and pressure scales, i.e., short times and high pressures versus long times and low pressures, both in cluster formation and chemical reactions. At the same time, the validity of our method has been questioned²⁴ because of discrepancies in detail between our results and those obtained from first principles for $n \leq 10$, and doubts have been raised once again as to the possibility of successful classical modeling of widely varying systems with a few-parameter classical field. We have therefore reexamined our expressions for the force field, especially its back-bonding component.

We find that with minor modifications of our previous potential we obtain an excellent fit to the first-principles results for Si_n with $3 \leq n \leq 10$ both as regards to the cluster energies and average bond lengths. Our modified potential gives much the same results for clusters with $n \geq 10$ and for surface or bulk defect energies as the old potential, as we expected, but now we are more confident of the overall accuracy of our approach.

II. CLASSICAL INTERATOMIC POTENTIAL FOR SILICON

The transcription of quantum-mechanical bonding properties for covalent solids into classical potential force fields is certainly nontrivial as our understanding of the covalent bond is far from complete. The process of transcription will no doubt be based on intuition instead of an analytic approach. Also, considering that quantum forces are nonlinear and nonlocal, we might expect some counter intuitive classical forces, e.g., larger three-body interactions than two-body interactions. Here we review briefly our previous work¹⁵ and define the modifications in our refined potential.

A. Defining a crystalline force field

The traditional approach to the problem of defining a force field appropriate for Si is usually based on the diamond structure and small perturbations away from this structure. For example, many of the potentials involve the interatomic vector \mathbf{R}_{ij} between the atoms i and j . The interactions are often based on the magnitude of this vector and the dot product $\mathbf{R}_{ij} \cdot \mathbf{R}_{jk}$. The key difference between our approach and that of previous force fields is that we choose our angular function in a physical, rather than a geometrical way. The explicit expression for our force field is

$$E[\{\mathbf{R}\}] = \sum_{\substack{i,j \\ i < j}} [A \exp(-\beta_1 R_{ij}^2)/R_{ij}^2 - g_{ij} \exp(-\beta_2 R_{ij}^2)/R_{ij}] . \quad (1)$$

R_{ij} is the interatomic distance between (i,j) and the many-body interactions are contained within the factor g_{ij} . We wish g_{ij} to be large for covalent systems (structures with large bond angles) as compared to metallic systems. We define g_{ij} as

$$g_{ij} = g_0 + g_1 S_{ij} S_{ji} , \quad (2)$$

where

$$S_{ij} = 1 + \langle \cos(3\theta_{ijk}) \rangle ,$$

$$\langle f(\theta_{ijk}) \rangle = [f]/[1] ,$$

$$[f(\theta_{ijk})] = \sum_{k \neq i,j} f(\theta_{ijk}) \exp(-\lambda_1 \theta_{ijk}^4) \exp(-\lambda_2 R_{ijk}^4) ,$$

with $R_{ijk} = (R_{ij} + R_{ik})/2$. θ_{ijk} is the angle formed by \mathbf{R}_{ij} and \mathbf{R}_{ik} . This form represents a very-short-ranged function which has sharp angular and radial cutoffs. The factor S_{ij} ranges from 0 for metallic structures with small bond angles to 2 for covalent systems. Also, for $\theta_{ijk} < \pi/3$ ($> 2\pi/3$) we saturate $\cos(3\theta_{ijk})$ so that $\cos(3\theta_{ijk}) = -1$ ($+1$). The parameters A , β_1 , β_2 , g_0 , and g_1 are determined by fitting the equation of state at $T=0$ K for various polytypes of silicon as determined by Cohen and co-workers.¹ Values for these parameters are given in Table I. Our potential yields one of the most accurate "classical" representations of the quantum-

TABLE I. Parameters for the interatomic potential as outlined in Eqs. (1)–(5). The parameters for the bulklike interactions are unchanged from previous work (Refs. 14 and 15).

Parameters for the bulk terms	
$A(\text{eV } \text{\AA}^{-2}) = 182.44$	$\beta_2(\text{\AA}^{-2}) = 0.151$
$\beta_1(\text{\AA}^{-2}) = 0.550$	$g_1(\text{eV } \text{\AA}) = 2.644$
$g_0(\text{eV } \text{\AA}) = 7.08$	$\lambda_1 = (2/\pi)^4$
$\lambda_2(\text{\AA}^{-4}) = 0.1733$	
Parameters for the dangling-bond terms	
$\lambda_3(\text{\AA}^{-4}) = 0.025$	$z(\text{\AA}^{-1}) = 0.0851$
$\mu = 11.0$	$\alpha = 1.4$

mechanical phase diagram for silicon to data. Even though we did not fit to the β -tin structure of the hcp structure, the pressure dependence and the structural parameters for these crystals are in good agreement with the quantum-mechanical results.

B. Dangling-bond corrections to the bulk force field

If we apply our potential in Eq. (1) to small silicon clusters, our results are not unexpected. We find the structure of Si_n ($n > 8$) resembles small fragments of the diamond structure as we have only included bulklike interactions. It is important to realize that such a finding implies that the ground-state crystal structure for our potential must be "diamondlike". This has not been the case for several other potentials. It is also important to note that the structure for Si_n is not in agreement with the findings of quantum chemistry. Quantum chemistry calculations have suggested the structure of Si_n resembles close-packed structures.^{16,17} Our bulk potential does not reproduce these results as we have not considered undercoordinated structures of silicon, i.e., "dangling-bond" structures. To remedy this situation, we must consider undercoordinated species.

Specifically, the transfer of bond strength from dangling to back bonds can produce more compact or more "metallic" structures. (We will call structures in which the average coordination exceeds four "metallic" and those structures for which the average coordination is less than or equal to four "covalent.") This transfer will depend on the angle θ_{ij} between the dangling bond and the back bond. We define a "dangling-bond vector" \mathbf{D}_i as follows:

$$\mathbf{D}_i = - \sum_{\substack{j \\ j \neq i}} \mathbf{R}_{ij} \exp(-\lambda_3 R_{ij}^4) / \sum_{\substack{j \\ j \neq i}} \exp(-\lambda_3 R_{ij}^4) . \quad (3)$$

For covalent systems, we expect large reconstructions. For metallic systems, we expect smaller reconstructions. We define a term to describe the back bonding as

$$Q_{ij} = 1 + z D_i \sin[\alpha(\theta_{ij} - \pi/3)] . \quad (4)$$

For crystalline systems, D_i vanishes and $Q_{ij} = 1$. In our previous work, we assumed for each interaction ij ,

$$\Delta g_0/g_0 = -\Delta g_1/g_1 = \mu(Q_{ij} Q_{ji} - 1) . \quad (5a)$$

The change vanishes for the crystalline case. This form assumes that the back-bond strengthening has the same range as the bulk interactions. Only the prefactors g_0 and g_1 are modified. While we obtained qualitatively correct structures for small clusters with this form, the bond lengths did not scale properly for low coordinated species. We noted in our previous paper¹⁵ that the bond lengths significantly increased for low coordinated species. Moreover, the bond lengths tended to be too large for the higher coordinated species. This was also verified by Andreoni and Pastore.²⁴

In order to correct this flaw in our potential, we have modified the dangling-bond correction so that our *new* form is as follows:

$$\begin{aligned} \Delta g_0/g_0 &= -\Delta g_1/g_1 \\ &= \mu(Q_{ij}Q_{ji} - 1)\exp(-\beta_2 R_{ij}^2). \end{aligned} \quad (5b)$$

As in our previous work, we have effectively separated the problem in two parts: crystalline structures and cluster structures. We need to determine four back-bonding parameters: z , α , μ , and λ_3 . Again, we used the molecular-orbital studies of Raghavachari and Rohlfing^{16,17} for the structural properties and energies of Si_n clusters with $n \leq 10$ to fix the parameters.

Physically we expect that the range of bonds altered by the presence of a dangling bond would not be equal to the range of the bulk interactions in Eq. (1). For example, the range of the perturbation of a surface in silicon, such as the ideal $\text{Si}(111)$ surface, is known to be significantly less than a few bond lengths. With our previous potential, the presence of the dangling bond resulted in all bonds being altered with a range determined by the Gaussian decay constant of β_2 . Since β_2 is determined purely by "bulklike" interactions, we cannot expect it to be accurate for cluster interactions. By choosing the form of Eq. (5b), we alter the range of the exponential by taking the decay constant of the dangling-bond correction to be twice β_2 . We tried other variations of this decay constant, but found that this value was optimal in terms of achieving accurate bond lengths for small Si clusters when compared to the quantum results. A significant alteration of our potential is that the value of μ must be altered to reflect the shorter range. We also found it necessary to change the value of α in Eq. (4) to preserve the original structures. Perhaps the most difficult parameter to adjust is λ_3 . This parameter controls the range of atoms which contribute to the dangling-bond vector. If the range is too short, we find that internal surfaces, or better, density fluctuations can occur. In our original potential, for larger clusters, i.e., $n \gtrsim 25$, we found internal voids could easily form. The potential in this situation takes advantage of surface creation without significant reduction of the bulk interactions. If we increase the range of this parameter, we suppress the formation of voids. At present, the available cluster data are not sufficient to fix λ_3 ; we need to know the structure for silicon clusters with $n > 20$. As a rough guide, we expect that $\lambda_3 \approx 1/R_M^4$ where R_M is the range of a metalliclike bond. In our previous potential, we used

a value for $R_M \approx 2.35 \text{ \AA}$, or the diamond bond length. In fcc silicon, this number corresponds to about $\approx 2.7 \text{ \AA}$, or $\lambda_3 = 0.02 \text{ \AA}^{-4}$. The value which we found preserved our previous results for the topology of the clusters, but did not introduce density fluctuations was $\lambda_3 = 0.025 \text{ \AA}^{-4}$. The previous value was $\lambda_3 = 0.033 \text{ \AA}^{-4}$. In summary, the new parameters for the back-bonding term are given in Table I.

III. STRUCTURAL PROPERTIES OF Si_n CLUSTERS WITH $n \leq 10$

Examining the structural properties of Si_n cluster with $n \leq 10$ offers some advantages in that these clusters have been studied via quantum chemistry,^{10,16,17} and pseudo-potential methods.^{18,19} These quantum-mechanical methods offer us a "standard" by which we can judge the merits of our interatomic force field results. Unfortunately, there are some inherent drawbacks to this procedure. Differences exist between some of the quantum results: notably between the generalized valence-bond approach of Messmer and co-workers¹⁰ versus the Hartree-Fock-based approach of Raghavachari and Rohlfing^{16,17} and the local density work.^{18,19} We have concentrated on the latter approaches as they form a consistent set. Another issue which complicates the problem is that small clusters often exhibit Jahn-Teller distortions and multiple bonds, which are not included in "classical" interatomic potentials. We cannot expect to obtain detailed, quantitative agreement with a force field approach for these small clusters. Our goal is more limited at this stage. Namely, we wish to obtain structures for Si_n cluster with $n \leq 10$ which are in "reasonable" agreement with the small clusters so that we may be able to predict the properties of larger clusters, e.g., $n > 20$. Our goal for these clusters is to obtain *plausible* structures which can then be examined in detail via more sophisticated approaches. Moreover, by construction, our potentials for large clusters must eventually converge to the correct crystalline structure as the surface correction will become a small perturbation for a sufficiently large cluster.

As with our previous work, we used a molecular-dynamics simulated annealing program to determine the lowest-energy structures.²⁵ At present it is not possible to explore large clusters with *ab initio* molecular dynamics. However, we can use simulation techniques to explore quite large clusters with our classical potentials. A standard Langevin-type equation of motion²⁵ is integrated using the interactions as outlined above. Initially, a random assemblage of atoms is considered. These atoms interact via our interatomic potential in a hypothetical viscous heat bath. The temperature of the bath is controlled so as to nucleate clusters from an initial high temperature. Details of this method are presented in our earlier work.¹⁵

In Fig. 1 we illustrate the binding energy per atom and the average bond length, normalized by the bulk crystal value, for silicon clusters with $n \leq 10$. By increasing the back-bonding strength via an increase in the value of the parameter μ , we increase the binding energy of the clusters as compared to our previous work. This is the case

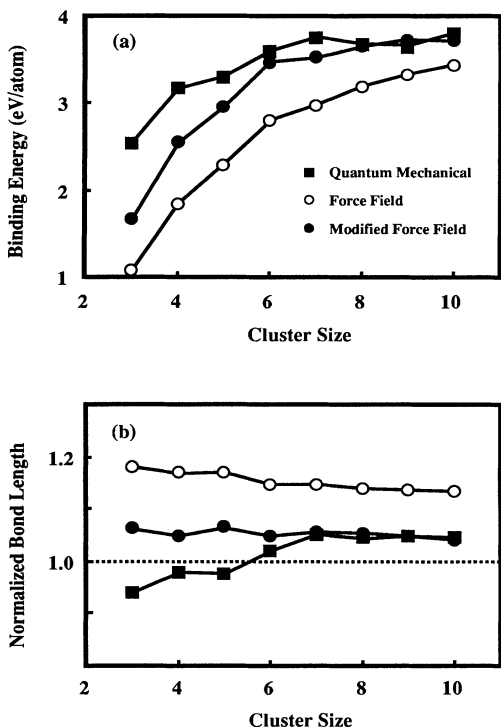


FIG. 1. Binding energies and the average bond length for Si_n clusters. The quantum-mechanical results for the binding energies (a) are from Raghavachari and Rohlfing (Refs. 16 and 17). The quantum-mechanical results for the average bond length (b) are from Andreoni and Pastore (Ref. 24). The modified force field work is from the present potential and the original force field work is from Refs. 14 and 15. The bond lengths were normalized to the bond length in the silicon diamond crystal.

even though the range of the interaction has been shortened in the new potential. As expected, the average bond length is shortened with an increased binding energy. For clusters, with $n \geq 6$, the agreement between the quantum results^{16,17} and our new potential is quantitative and a considerable improvement over the previous potential. However, for $n < 6$ significant differences remain. The bond lengths are too long compared to quantum-mechanical calculations²⁴ and the binding energy is considerably less. This is *not* a surprising result. As in our previous work, we found that for low coordinated Si species, the bond length increases instead of decreasing as one might expect. The traditional chemical explanation for this effect is that “double” bonds can form for undercoordinated species, e.g., the Si dimer has a shorter bond length than the bond length in the silicon diamond crystal. As noted elsewhere,²⁴ one expects such a result for a classical potential such as a Lennard-Jones potential. Since we have not included “double” bonds, or similar “quantum” effects, we cannot expect our potential to reproduce the quantum results in such situations.

Another comparison which can be made with quantum calculations concerns the size dependence of the fragmentation energy. We define the fragmentation energy E_{fr} as

$$E_{\text{fr}} = E(n) - [E(n-m) + E(m)], \quad (6)$$

where the choice of m minimizes E_{fr} . This expression does not include the effects of kinetics; we compare here the equilibrium differences between the most stable clusters as function of size.

The details of the fragmentation process which involve products Si_n where $n < 6$ are not expected to be represented with high accuracy. The energy for these clusters is not well reproduced by interatomic potentials. In general, we underestimate the binding energy of such clusters. Thus for $n < 12$, all Si_n clusters determined by our potential will fragment into Si_{n-1} and a monomer. However, if we examine the fragmentation energies involved without regard to details of the fragmentation process, our results are credible. In Fig. 2 we compare our calculated values with the fragmentation energies as determined by quantum chemistry.^{16,17} The fragmentation energies for these clusters have also been examined via pseudopotential–local-density methods^{18,19} with results similar to the quantum chemistry work. As expected, the primary difference between the quantum chemistry and the pseudopotential–local-density method is that the latter produces larger binding energies and fragmentation energies. This difference can be as large as $\sim 1-2$ eV. Since we have constructed our potentials to reproduce the quantum chemistry work, we compare to these results.

The largest discrepancy between our fragmentation energy and the quantum chemistry work concerns the fragmentation of Si_8 . We note that the energy for fragmenting Si_8 exceeds that of Si_7 and Si_9 which is contrary to both the quantum chemistry and pseudopotential–local-density work. This discrepancy is not confined to our interatomic potential, but is true for the work of Tersoff⁴ and that of Bolding and Andersen.¹³ Interestingly, the quantum work and our potential yield very similar structures for Si_7 and Si_8 . Si_7 is a bicapped pentagonal structure and Si_8 is a bicapped octahedron. In our calculation, this octahedron is capped on adjacent faces. In the

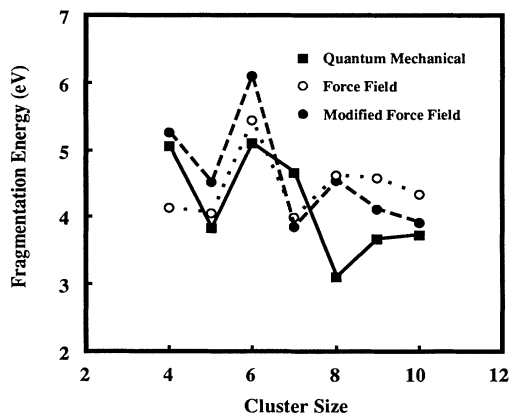


FIG. 2. Fragmentation energies for small clusters as defined by Eq. (6). The quantum results are from Raghavachari and Rohlfing (Refs. 16 and 17). The original force field is from Refs. 14 and 15. The modified force field is from the present interatomic potential.

quantum calculation, opposite faces are capped. It is possible that the difference in structural energies is a true “quantum” effect. Namely, Jahn-Teller distortions are known to exist for the eight-atom structure. If this distortion were to lower the energy of the cluster by ~ 0.1 eV/atom, then the discrepancy between our classical potential and the quantum work would be eliminated.

In terms of the detailed structures for the clusters, we retain the same topology as obtained with our previous potential. For the most part, these structures are similar to the quantum-mechanical results.^{16,17} However, some notable differences occur. For example, Si_3 is an equilateral triangle; the quantum structure is not equilateral, but has a base angle of 80° . Our structure for Si_4 is a tetrahedron whereas the quantum chemistry results are planar. For $\text{Si}_{5,6}$ we find symmetric, close-packed structures while the quantum chemistry work suggests that the structures are distorted by Jahn-Teller forces. However, we agree for Si_7 and our structures for Si_{8-10} are “competitive,” i.e., they lie close in energy to the quantum chemistry ground-state structures. As discussed by Andreoni and Pastore,²⁴ the classical structures tend to be separated by larger energy differences than the quantum results. This is not a surprising result. For a classical potential, the variables which determine the energy are equal to the physical degrees of freedom, i.e., the set of position vectors: $\{\mathbf{R}_{ij}\}$. Quantum mechanically, the degrees of freedom are represented by the wave-function manifold, i.e., a many-body wave function: $\psi(\mathbf{R}_1, \mathbf{R}_2, \dots; \mathbf{r}_1, \mathbf{r}_2, \dots)$ with the electronic coordinates given by \mathbf{r}_i . One would expect these extra electronic degrees of freedom to yield a lower ground state energy and reduce differences in the structural energies as compared to a purely classical description.

IV. STRUCTURAL PROPERTIES OF Si_n CLUSTERS WITH $10 < n \leq 30$

As the cluster size increases, several difficulties become manifest. The number of competing structures is no longer small; it becomes impractical to create an inventory of structures. Statistical methods become necessary to explore possible ground-state structures. Moreover, we are unable to compare to results from quantum-mechanical methods. For Si_n , $n \gtrsim 10$, no quantum results exist at present as the number of atoms in the cluster precludes *ab initio* methods for determining total energies except for special candidate structures. We expect our method to be most successful for this regime.

In Fig. 3 we plot the binding energy for our clusters as a function of size. One expects that the “binding energy versus size” curve will be converged better than the specifics of the structural properties of an individual cluster. On the scale shown in this figure, the increase with size is linear. For a larger span of cluster size, one might expect to see an $n^{1/3}$ correction if bulk terms dominate. If we fit our calculated values of $E(n)$ vs n to $E(n) = a + bn$, we find $a = -5.52$ eV and $b = 4.27$ eV/atom. Since $b = \lim_{n \rightarrow \infty} [E(n)/n]$ corresponds to the binding energy for an infinitely large cluster, one can

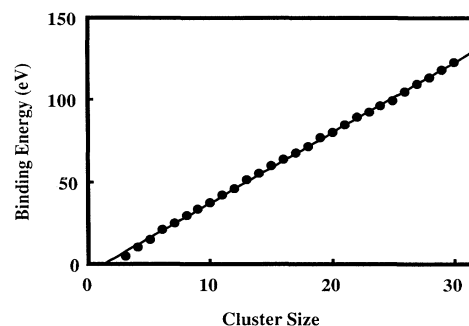


FIG. 3. The binding energy of Si_n clusters for $n \leq 30$.

compare this to the cohesive energy of silicon in the diamond structure. The cohesive energy of silicon is 4.63 eV/atom or about 8% larger than the value extrapolated from Fig. 3. Since the number of surface atoms for these clusters is a significant fraction of the total number in the cluster, we expect a value lower than that for the crystal.

In Fig. 4 we plot the binding energies per silicon atom. The nature of the structures is reflected in the icosahedral behavior of the cluster at $n = 13$ and 19 where an abrupt increase in the binding energy is observed. For Si_n where $n > 20$, the pentagonal growth structure is not reflected in a characteristic increase in the binding energy of $n = 23$ which would be the next “special” structure. This is also reflected in the experimental work of Jarrold and co-workers.^{20,23} Si_{13} and Si_{19} exhibit little reactivity with ethylene, oxygen, or water as contrasted with other cluster size, but no special behavior was observed for larger clusters.

In Fig. 5 we illustrate the average coordination as a function of cluster size. This measure of the structure is only a rough guide as it is difficult to define a precise definition of a “bond.” We have used a cutoff of 2.7 \AA , but the results are somewhat sensitive to the cutoff employed. For Si_n , $n < 10$, we find a monotonic increase of

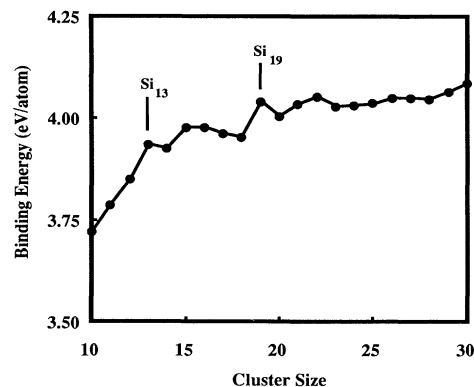


FIG. 4. The binding energy per atom for Si_n clusters for $10 \leq n \leq 30$. We find special structures at $n = 13$ and 19 as expected for icosahedral cluster growth. The crystalline cohesive energy is 4.63 eV/atom.

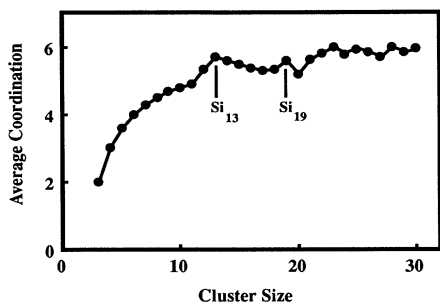


FIG. 5. The average coordination per atom for Si_n clusters for $n \leq 30$. We find special structures at $n = 13$ and 19 as expected for icosahedral cluster growth.

coordination with cluster size. At $n = 13$ there is a local maxima for the icosahedral structure. After the completion of the icosahedra, the coordination tends to decline as we cap off the core structure until the “double” icosahedra forms at $n = 19$. For $n > 20$, the icosahedral structure remains a building block, but the structures are less regular.

In Fig. 6 we illustrate the fragmentation energy as a function of cluster size. The structures at $n = 4, 6, 13, 15,$ and 19 are particularly stable against fragmentation. A general decline in the fragmentation energy is noticeable, particularly above $n = 20$. One might speculate as to whether the clusters in this size regime are approaching a transition to a different type of cluster structure, e.g., one somewhat removed from an icosahedral-based scheme. An issue open to conjecture is at what size the icosahedral, or close-packing, geometry becomes unstable against a more open, “diamondlike” cluster. As one increases the cluster size, we expect such a transition as the binding energy per atom for the diamond crystal is significantly larger (see Fig. 4) than for the cluster geometry in this regime. In Fig. 7 we illustrate the structure of the clusters for $n > 20$. For $n \leq 20$, the structures are similar to those determined by our earlier work. Icosahedral units are apparent in the structures, but the

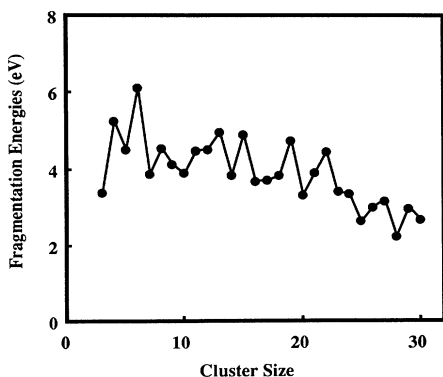


FIG. 6. Fragmentation energies for Si_n clusters for $n \leq 30$. The fragmentation energies are defined by Eq. (6).

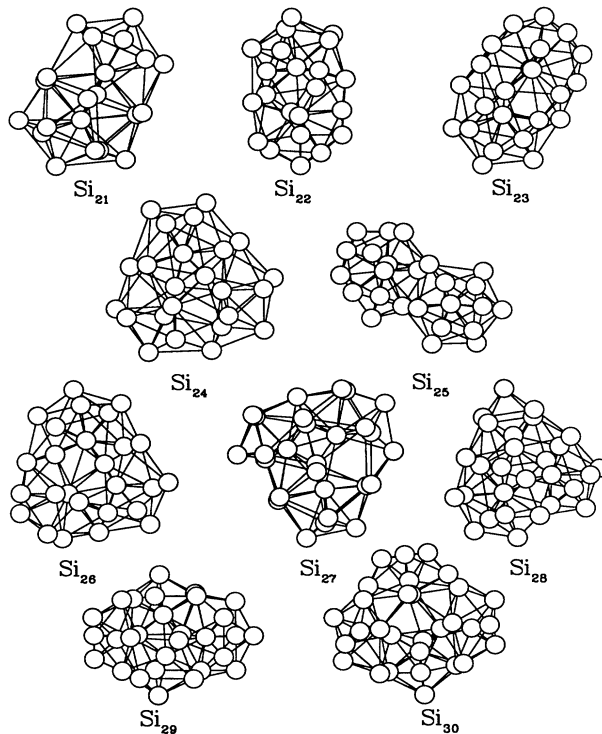


FIG. 7. Structures for Si_n for $21 \leq n \leq 30$.

structures do not correspond to a simple “capping” off of the surfaces of the double icosahedra for $n > 22$.

V. THE ROLE OF BACK-BONDING IN SILICON CLUSTERS: FIRST-ORDER COVALENT TO METALLIC STRUCTURAL TRANSITIONS

One advantage we have in using empirical potentials is that we can easily vary potential parameters and gain insights into how various structures form. A key issue is the transition with back bonding strength from “under-coordinated” to “over-coordinated” clusters: from clusters with less than four bonds per neighbor to clusters with more than four bonds per neighbor. A parameter which dominates this “under-coordinated” to “over-coordinated” transition is the parameter μ in Eq. (5b). If we set this parameter to zero, under-coordinated structures are produced as only bulk interactions are present. As we increase this parameter, eventually the back bonds are strengthened to such an extent that the structure “switches” over to an “over-coordinated” structure. The nature of this transition is of some interest. In the construction of the potential, we included an explicit “metal”-to-“semiconductor” transition into the nature of the bonding. This “semiconductor-to-metal” transition occurs in the behavior of silicon under pressure where the change is from a fourfold structure (diamond) to a sixfold structure (white tin). It also occurs in the melting transitions where silicon transforms from a semiconductor solid to a metallic liquid with an average coordination on

the order of 5. Both of these transitions are first order with an abrupt change in the coordination.

We hope to model our potential to obtain similar behavior in our clusters. By increasing the back-bonding strength, we expect to find an abrupt change from a semiconductor structure where the average coordination is less than four to a metallic structure where the average coordination is greater than four. For all the clusters we have examined, we find that there is a narrow region in parameter space where this change from covalent to metallic structures occurs. In Fig. 8 we illustrate the average coordination for Si_n where $n = 5, 10, 15, 20, 25$, and 30. Determining a criterion for the average coordination here is nontrivial. We used a larger cutoff than for the average coordination in Fig. 6. When we alter the dangling-bond interactions, the bond length may change; however, the topology of the cluster does not. By using a larger cutoff ($\sim 3 \text{ \AA}$), we represent changes in the topology better than if we use a smaller cutoff. Also, we start each cluster from the same initial configuration so that changes in the interaction parameter will dominate the changes in structure. Nonetheless, our annealing process is statistical and small random changes in the structure

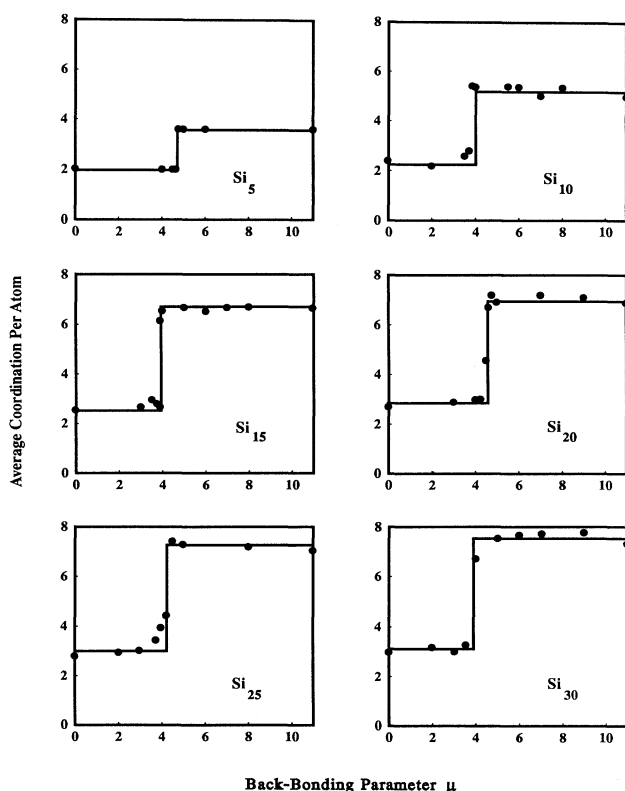


FIG. 8. Variation of cluster structure as measured by the average coordination with the back-bonding parameter μ as defined in Eq. (5b). Illustrated is the average coordination for clusters, Si_{5m} , for $m = 1, 2, \dots, 6$. The lines are a guide to the eye and illustrate the abrupt change in coordination which occurs with back-bonding strength.

occur which result in differences in the average coordination. This is evident in the behavior of Si_{10} which exhibits coordination fluctuations with changing values of μ . However, the topology of the cluster structure of Si_{10} is not significantly altered.

We consider changes from $\mu = 0$ to 11. Small values of μ result in a covalent network, i.e., fivefold sixfold rings. For $\mu \approx 4-5$, we see an abrupt change in the coordination. For larger values of μ , the cluster becomes metallic, i.e., coordination greater than four. In Fig. 9 we illustrate these structures for a Si_{20} cluster. For $\mu = 0$ the cluster is open with an average coordination near 2. As we increase μ to a value near 4, we find a structure which has characteristics of both a close-packed structure and an open structure. Part of the Si_{20} structure has nucleated a metallic "seed" which appears similar to a bicapped pentagonal structure as we found for Si_7 . For large values of μ , the cluster has become close packed. The rapid transition between open and close-packed structures is "first order" in the sense that it occurs abruptly as a function of μ . Just as for a true "first-order" transition, we find some fluctuations near the transitions region. No doubt many of these fluctuations are kinetic in that if we annealed for a longer period of time, the transition might be even sharper.

As the cluster size grows, we expect that eventually the crystalline environment must be obtained. For small clusters, the surface term is dominant and a fairly small value of μ will change the structure of the cluster from covalent to metallic. However, for sufficiently large clusters, the volume term will dominate. For the surface term to drive the cluster into a metallic structure, a large value of μ will be required. The value of the transition for Si_{10} is about $\mu = 4$ and for Si_{20} is about $\mu = 4.5$. If we were to infer a value of n_c which would correspond to a covalent

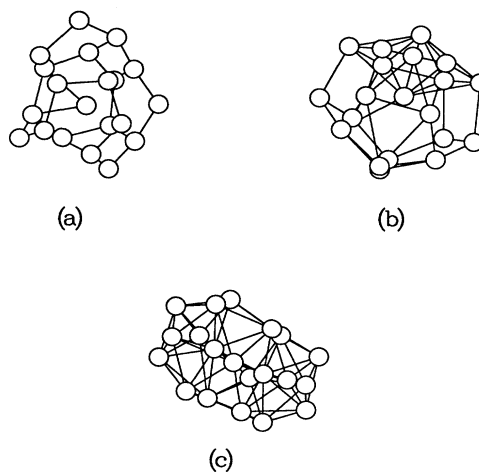


FIG. 9. Structure for Si_{20} as function of the back-bonding parameter. The three structures shown correspond to (a) no back-bonding term ($\mu = 0$), (b) the structure at the transition (Fig. 8) ($\mu = 4.5$), and (c) the structure for the assumed value of the back-bonding strength ($\mu = 11$).

structure for Si_n , we expect on the basis of a crude extrapolation for $n_c \approx 100$. At this point, $\mu \approx 10$ would result in a covalent structure. Unfortunately, the cluster size range we examine here is not large enough for us to make a quantitative estimate of this trend. In fact, $n = 5$ has a higher transition value for μ and the transitions for other values of n are not so well defined as for $n = 10$ or 20. Quantitative estimates for the cluster size at which the transition from a close-packed cluster to an open structure takes place have ranged from $n \approx 10^2 - 20^3$. Most of the estimates are in the range $n \approx 50 - 100$, which is consistent with our work here.²⁶

VI. CONCLUSIONS

We have constructed an interatomic potential for silicon. This potential is similar to our previous work as it is based on bulk interactions which were adjusted to describe "covalent \rightarrow metallic" phase transitions instead of small-amplitude atomic vibrations. It includes the transfer of bond strength from dangling bonds to back bonds. However, our new potential has been slightly modified so that the range of such dangling-bond corrections is shorter than that of the bulk interactions.

We applied this potential to Si_n clusters where $n \leq 30$. Molecular dynamical simulations were used to nucleate clusters. For $n \leq 10$ we found that this potential led to a significant improvement over previous work for both the binding energies and the bond lengths of these clusters when compared to quantum-mechanical methods. For

$10 < n \leq 20$ we found in agreement with experiment, and with our previous work, that Si_n clusters follow an icosahedral pentagonal growth sequence with $n = 13$ and 19 being special structures, i.e., icosahedral structures. For $20 < n \leq 30$ we found that this growth pattern is weakened, but elements of pentagonal growth sequence are retained.

One major advantage of our approach is that we are able to vary the back-bonding interactions and control whether the structure is open or close packed. For small values of the back-bonding interaction, the cluster is open. As the strength of the back-bonding parameter is increased the cluster undergoes an abrupt change from an open to a close-packed structure. We found that this transition is first order in nature and occurs over a very limited range of parameter space. Thus, "covalent \rightarrow metallic" transition of the clusters mimic the behavior of the crystalline forms of silicon. Our ability to vary this interaction will allow us to examine fundamental differences between covalent and metalliclike clusters.

ACKNOWLEDGMENTS

We (J.R.C. and K.M.G.) would like to acknowledge support for this work by the U.S. Department of Energy of the Office of Basic Energy Sciences (Division of Materials Research) under Grant No. DE-FG02-89ER45391. We would also like to acknowledge computational support from Cray Research and the Minnesota Supercomputer Institute. One of us (J.R.C.) wishes to acknowledge the hospitality of AT&T Bell Laboratories.

-
- ¹M. T. Yin and M. L. Cohen, Phys. Rev. B **26**, 5668 (1982); K. J. Chang and M. L. Cohen, *ibid.* **31**, 7819 (1985).
²F. Stillinger and T. Weber, Phys. Rev. B **31**, 5262 (1985).
³R. Biswas and D. R. Hamann, Phys. Rev. Lett. **55**, 2001 (1985); Phys. Rev. B **36**, 6434 (1987).
⁴J. Tersoff, Phys. Rev. Lett. **56**, 632 (1986); P. C. Kelires and J. Tersoff, *ibid.* **61**, 562 (1988).
⁵B. W. Dodson, Phys. Rev. B **35**, 2795 (1987).
⁶M. I. Baskes, Phys. Rev. Lett. **59**, 2666 (1987).
⁷E. Blaisten-Barojas and D. Levesque, Phys. Rev. B **34**, 3910 (1986).
⁸B. Feuston, R. K. Kalia, and P. Vashista, Phys. Rev. B **37**, 6297 (1988).
⁹S. Saito, S. Ohnishi, and S. Sugano, Phys. Rev. B **33**, 7036 (1986).
¹⁰C. H. Patterson and R. P. Messmer, Phys. Rev. B **42**, 7530 (1990); R. P. Messmer, W. -X. Tang, and H. -X. Wang, *ibid.* **42**, 9241 (1990).
¹¹E. Kaxiras, Phys. Rev. Lett. **64**, 551 (1990).
¹²A. D. Mistriotis, N. Flytzanis, and S. C. Farantos, Phys. Rev. B **39**, 1212 (1989).
¹³B. C. Bolding and H. C. Andersen, Phys. Rev. B **41**, 10568 (1990).
¹⁴J. R. Chelikowsky, J. C. Phillips, M. Kamal, and M. Strauss, Phys. Rev. Lett. **62**, 292 (1988).
¹⁵J. R. Chelikowsky and J. C. Phillips, Phys. Rev. Lett. **63**, 1653 (1989); Phys. Rev. B **41**, 5735 (1990).
¹⁶K. Raghavachari, J. Chem. Phys. **83**, 3520 (1985); **84**, 5672 (1986).
¹⁷K. Raghavachari and C.M. Rohlfing, J. Chem. Phys. **89**, 2219 (1988).
¹⁸D. Tomanek and M. Schluter, Phys. Rev. Lett. **56**, 1055 (1986); Phys. Rev. B **36**, 1208 (1987).
¹⁹P. Ballone, W. Andreoni, R. Car, and M. Parrinello, Phys. Rev. Lett. **60**, 271 (1988).
²⁰M. F. Jarrold, J. E. Bower, and K. Creegan, J. Chem. Phys. **90**, 3615 (1989); M. F. Jarrold, U. Ray, and K. M. Creegan, *ibid.* **93**, 224 (1990), and references therein.
²¹J. L. Elkind, J. M. Alford, F. D. Weiss, R. T. Laaksonen, and R. E. Smalley, J. Chem. Phys. **87**, 2397 (1987).
²²S. Maruyama, L. R. Anderson, and R. E. Smalley (unpublished).
²³U. Ray and M. F. Jarrold, J. Chem. Phys. **93**, 5709 (1990).
²⁴W. Andreoni and G. Pastore, Phys. Rev. B **41**, 10243 (1990).
²⁵See J. C. Tully, G. H. Gilmer, and M. Shugard, J. Chem. Phys. **71**, 1630 (1979), and Ref. 3.
²⁶J. R. Chelikowsky, Phys. Rev. Lett. **60**, 2669 (1988), and references therein.